Magn Reson Med Sci 2017; 16; 245–252
doi:10.2463/mrms.mp.2016-0037 Published Online: November 16, 2016

MAJOR PAPER

Diagnostic Performance of Diffusion Tensor Imaging with Readout-segmented Echo-planar Imaging for Invasive Breast Cancer: Correlation of ADC and FA with Pathological Prognostic Markers

Ken Yamaguchi[1*], Takahiko Nakazono[1], Ryoko Egashira[1], Yoshiaki Komori[2], Jun Nakamura[3], Tomoyuki Noguchi[1,4], and Hiroyuki Irie[1]

Purpose: To assess the diagnostic performance of readout-segmented echo-planar diffusion tensor imaging (DTI based on rs-EPI) for breast cancer and to determine the correlation between the apparent diffusion coefficient (ADC) and fractional anisotropy (FA) values obtained from DTI based on rs-EPI with prognostic markers of invasive breast cancer.

Materials and Methods: This retrospective study examined 80 pathologically proven breast lesions (22 benign and 58 malignant lesions) of 80 patients who underwent both diffusion-weighted imaging based on single-shot echo-planar imaging (DWI based on ss-EPI) and DTI based on rs-EPI with b-values of 0 and 1000. We identified and compared the diagnostic performances of the DWI based on ss-EPI and the DTI based on rs-EPI using ADCs by conducting a receiver-operating-characteristics (ROC) analysis. We determined the correlations between the ADCs and the prognostic markers and those of the FA values and the same markers.

Results: The median ADCs of the benign and malignant lesions based on the ss-EPI were 1.57 and 1.2×10^{-3} mm^2/sec, and those based on the rs-EPI were 1.53 and 1.09×10^{-3} mm^2/sec, respectively. The area under the curve on the ROC analysis based on rs-EPI (0.924) was greater than that based on ss-EPI (0.897). There were no significant correlations between the ADCs and the prognostic markers, but there were significant correlations between the FA values and the estrogen receptor status, a proliferative marker, the nuclear grade and the intrinsic subtype.

Conclusion: For breast cancer, DTI based on rs-EPI had superior diagnostic performance compared to DWI based on ss-EPI. Compared with the ADCs, the FA values were more closely correlated with prognostic markers of invasive breast cancer.

Keywords: *breast, MRI, diffusion-weighted imaging, readout-segmented echo planar imaging, diffusion tensor imaging*

Introduction

Breast magnetic resonance imaging (MRI) has become an important tool in the evaluation of various breast lesions and conditions, including the diagnosis and staging of breast cancer.[1–6] Breast MRI has been performed based mainly on a post-contrast dynamic sequence with the use of contrast-enhancement materials. Diffusion-weighted imaging (DWI) of the breast can detect breast cancer without the need for contrast-enhanced materials.[7–10] DWI findings can be obtained for patients who have contraindications for contrast-enhanced MRI such as poor renal function and allergy to contrast-enhanced materials.

However, the image quality of DWI is lower than that of typical dynamic contrast images for several reasons, including geometric distortions, image blurring, ghost artifacts and the problem of fat suppression.[7,11,12] Diffusion-weighted images are usually made from single-shot echo-planar imaging (ss-EPI). DWI based on readout-segmented echo-planar imaging (rs-EPI)

[1]Department of Radiology, Faculty of Medicine, Saga University, 5-1-1 Nabeshima, Saga 849-8501, Japan
[2]Siemens Japan K.K. Research & Collaboration Department, Tokyo, Japan
[3]Department of Surgery, Faculty of Medicine, Saga University, Saga, Japan
[4]Department of Radiology, National Center for Global Health and Medicine (NCGM), Tokyo, Japan

*Corresponding author, Phone: 81-952-34-2309, Fax: 81-952-34-2016, E-mail: yamaguk@cc.saga-u.ac.jp

Received: November 17, 2015 | Accepted: September 9, 2016

has begun to be used in clinical settings involving breast cancer.[12–14] This technique is designed to provide improved image quality compared to ss-EPI with the use of two-dimensional navigator phase correction sequences to minimize the motion artifact,[15] and the rs-EPI technique was reported to reduce geometric distortions, image blurring and ghost artifact.[12–14]

Diffusion tensor imaging (DTI) for the breast has been reported.[16–23] DTI represents an extension of standard DWI with diffusion encoding in at least six directions, and it can measure the full diffusion tensor and characterize the motion of water in more detail.[16–18] In addition to apparent diffusion coefficient (ADC) values, DTI provides measures of diffusion anisotropy (fractional anisotropy, or FA).[16–18] Several studies reported the results of quantitative analyses of breast lesions with the use of FA values in DTI.[17–20,22]

To our knowledge, only a few studies have compared the diagnostic performance between DWI based on ss-EPI and that based on rs-EPI.[12,13] In addition, although several studies have described the diagnostic performance of DTI for breast cancer,[18–20] no study has established the relationship between DTI findings and prognostic markers of breast cancer. We designed a new DWI technique that combines rs-EPI and DTI to obtain both ADC and FA values with image quality that is improved compared to that obtained with ss-EPI. The purposes of the present study were to assess the diagnostic performance of readout-segmented echo-planar DTI (DTI based on rs-EPI) for breast cancer and to determine the correlation between ADC and FA values obtained from DTI based on rs-EPI with prognostic markers of invasive breast cancer.

Materials and Methods

Patients

This retrospective study was approved by the institutional review board at our institution, and written informed consent was waived. Between June 1, 2013 and September 1, 2015, 62 cases of breast cancer were confirmed by surgery in 62 women who underwent breast MRI at our institution. Of these patients, four underwent the surgery after neoadjuvant chemotherapy, and these four cases were excluded from the present analyses. During the same period, 27 cases of benign breast lesions were demonstrated by biopsy or surgery in 27 women who underwent breast MRI. Of these 27 patients, five breast lesions were not detected on DWI images due to their small size, and these five cases were excluded from our analysis. Thus, a total of 80 pathologically proven breast lesions (22 were benign and 58 were cancer) from 80 women (median age: benign; 46 years, cancer; 62.5 years) were examined in this study.

MRI technique

During the study period, all examinations were performed using a 1.5T MR system (MAGNETOM Avanto, Siemens Healthcare, Erlangen, Germany) with a dedicated two-channel breast coil. The imaging protocol obtained axial short-tau inversion-recovery (STIR) T_2-weighted images (TR/TE, 7100/76; flip angle, 160°; echotrain length, 11; acquisition matrix size, 140 × 140; slice thickness, 6 mm; field of view [FOV], 350 mm), axial spin echo T_1-weighted images (TR/TE, 633/8.4; echotrain length, 1; acquisition matrix size, 140 × 140; slice thickness, 6 mm; FOV, 350 mm), axial diffusion-weighted images based on ss-EPI (TR/TE, 5500/75; parallel imaging, GRAPPA2; echo spacing, 0.69; acquisition matrix size, 140 × 140; slice thickness, 5 mm; FOV, 350 mm; fat suppression, STIR method; acquisition time, 2 min 52 s), axial diffusion tensor images based on rs-EPI (TR/TE, 3000/69; parallel imaging, GRAPPA2; echo spacing, 0.34; acquisition matrix size, 140 × 140; slice thickness, 5 mm; FOV, 350 mm; fat suppression, chemical shift selective (CHESS) method; acquisition time, 3 min 8 s; diffusion directions, six directions and readout-segments, 7).

Both diffusion protocols were acquired at the b-values of 0 and 1000 s/mm^2. Subsequently, one pre-contrast and five dynamic post-contrast enhanced axial T_1-weighted image sets with a 3D gradient-echo sequence with fat suppression (TR/TE, 3.42/1.4; flip angle, 6×; echotrain length, 1; acquisition matrix size, 140 × 140; slice thickness, 2 mm; FOV, 350 mm).

An ADC map was created automatically by the MRI console in both the DWI based on ss-EPI and the DTI based on rs-EPI technique. An FA map was also created automatically by the MRI console in the DTI based on rs-EPI technique.

Pathology

All pathology data were based on pathological reports. Of the 58 breast cancer lesions, there were 43 cases of invasive ductal carcinoma (IDC), five cases of invasive lobular carcinoma (ILC), two cases of mucinous carcinoma or IDC with mucinous component, one case of invasive micropapillary carcinoma, one case of tubular carcinoma, one case of apocrine carcinoma, and five cases of ductal carcinoma in situ (DCIS). The median size of these breast cancer lesions was 19.5 mm (range 6–90 mm). The 53 invasive breast cancer lesions were classified into four intrinsic subtypes according to the St. Gallen International Expert Consensus 2013.[24] Of the 53 cases, 28 were classified as luminal A-like type, 10 were classified as luminal B-like type, four were classified as human epidermal growth factor receptor 2 (HER2) positive type, and 11 cases were classified as triple-negative (TN) cancer.

Among the 22 benign breast lesions, there were four cases of fibroadenoma, four of mastopathy, three of intraductal papilloma, three cases of adenosis, two of ductal and lactating adenoma, one benign phyllodes tumor, one pseudoangiomatous stromal hyperplasia, one focal ductal hyperplasia, two cases of hemorrhage and inflammatory change and one case of fibrotic change. The median size of these benign lesions was 15 mm (range 10–60 mm).

Assessment of ADCs and FA values and the statistical analyses

For the assessment of ADCs and FA values, one radiologist (K.Y.) manually traced the region of interest (ROI) in the

breast cancer and benign breast lesions on DWI. Each ROI was placed over as much of the lesion as possible on the slice showing the maximum diameter. Each ROI was then copied to the ADC and FA maps, and the ADC and FA value of each lesion were calculated. These ADCs and FA values were assessed on a dedicated workstation (AZE VirtualPlace, AZE, Tokyo, Japan). Pathology data were blinded during this assessment. The patient information including pathology results was collected from our hospital's electronic medical records and Picture Archiving Communication System (PACS).

For the statistical evaluation, we used Shapiro-Wilk's test to determine whether or not the data were normally distributed. We used the Mann–Whitney test to analyze the relationship between ADCs and malignancy. We performed a receiver operating characteristic (ROC) analysis to evaluate the diagnostic performance of the ADCs in both the DWI based on ss-EPI and the DTI based on rs-EPI. Our evaluation of the relationship between FA values and malignancy was also performed with the Mann–Whitney test.

To evaluate the relationships between both ADCs and FA values with prognostic markers of invasive breast cancer, we used the following parameters: estrogen receptor (ER) (positive vs. negative), progesterone receptor (PgR) (positive vs. negative), human epidermal growth factor receptor 2 (HER2) (positive vs. negative), a proliferative marker (the Ki67 labeling index: percentage), the nuclear grade (grades 1 and 2 vs. grade 3), the intrinsic subtype (luminal A and B-like type vs. HER2-positive type and TN cancer) and lymph node (LN) status (positive vs. negative).

For the DWI based on ss-EPI, we used the Mann-Whitney test for the statistical evaluation of the relationship between ADCs and the ER status, PgR, HER2, nuclear grade, and intrinsic subtype. We used *t*-test to evaluate the relationship between ADCs and the LN status, and Spearman's rank correlation test to evaluate the relationship between ADCs and the Ki67 labeling index (the proliferative marker).

For the DTI based on rs-EPI, we used t-test to evaluate the relationships between ADCs and the following parameters: the ER status, PgR, HER2, nuclear grade, intrinsic subtype and LN status. We evaluated the relationship between ADCs and the Ki67 labeling index with Pearson's correlation test. The relationships between the FA values and the ER status, PgR, HER2, nuclear grade, intrinsic subtype and LN status were evaluated using the Mann–Whitney test. We used Spearman's rank correlation test to determine the relationship between FA values and the Ki67 labeling index. *P*-values <0.05 were considered significant. The PASW statistics 18 software package (SSPS, Chicago, IL) was used for all analyses.

Results

As summarized in Table 1, the mean (median) ADCs of the benign and cancer lesions revealed by DWI based on ss-EPI were 1.99 (1.57) and 1.2 (1.2), respectively. The mean (median) ADCs of the benign and cancer lesions revealed by DTI based on rs-EPI were 1.51 (1.53) and 1.11 (1.09), respectively. The ADCs calculated from DTI based on rs-EPI tended to be lower than those from DWI based on ss-EPI (Table 1). With both techniques, the ADCs of the breast cancers were significantly lower than those of the benign lesions ($P < 0.001$ for both techniques) (Table 1).

Table 1. ADCs obtained by DWI based on ss-EPI and by DTI based on rs-EPI

		Mean (median) ± SD	*P*-value
DWI based on ss-EPI	benign	1.99 (1.57) ± 2.06	
	breast cancer	1.2 (1.2) ± 0.22	<0.001
DTI based on rs-EPI	benign	1.51 (1.53) ± 0.22	
	breast cancer	1.11 (1.09) ± 0.22	<0.001

ADCs are given in $\times 10^{-3}$ mm^2. SD, standard deviation.

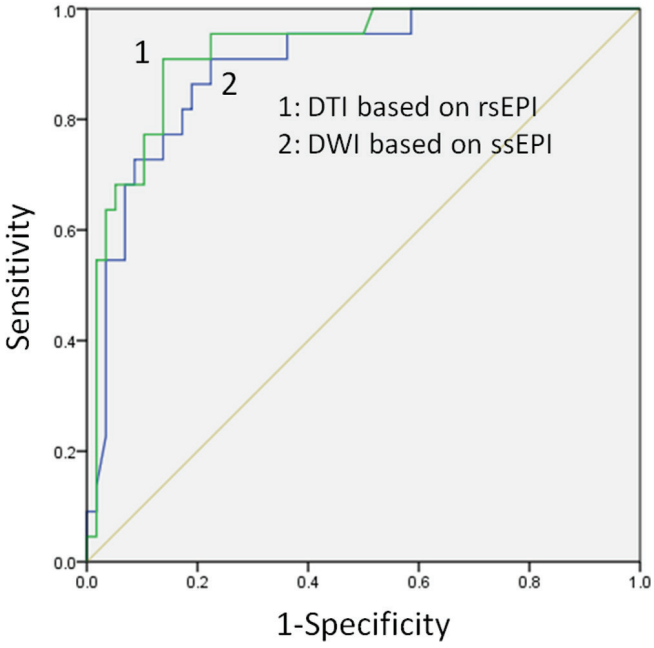

Fig 1. The AUC based on readout-segmented EPI (0.924) was greater than that based on single-shot EPI (0.897).

The ROC analysis showed that the area under the ROC curve (AUC) of the DWI based on ss-EPI was 0.897 (Fig. 1), and at the cutoff ADC value of 1.353, the sensitivity and specificity for diagnosing breast cancer were 86% and 81%, respectively. The AUC of the DTI based on rs-EPI was 0.924 (Fig. 1). At the cutoff ADC value of 1.338, the sensitivity and specificity for diagnosing breast cancer by this technique were 91% and 86%, respectively. The AUC based on rs-EPI (0.924) was thus greater than that based on ss-EPI (0.897) (Fig. 1).

There were no significant correlations between the ADCs and any of the prognostic markers in the DWI based on ss-EPI or the DTI based on rs-EPI (Tables 2, 3).

Table 2. ADCs obtained with DWI based on ss-EPI regarding the prognostic markers

		Mean (median) ± SD	*P*-value
ER	positive	1.19 (1.14) ± 0.25	0.612
	negative	1.2 (1.2) ± 0.17	
PgR	positive	1.2 (1.15) ± 0.25	0.985
	negative	1.18 (1.19) ± 0.17	
HER2	positive	1.16 (1.13) ± 0.15	0.792
	negative	1.2 (1.18) ± 0.24	
Nuclear grade	grades 1, 2	1.22 (1.19) ± 0.23	0.247
	grade 3	1.11 (1.1) ± 0.18	
Intrinsic subtype	luminal type	1.2 (1.15) ± 0.24	0.984
	HER2-positive, TN	1.18 (1.2) ± 0.18	
LN status	positive	1.14 (1.12) ± 0.17	0.249
	negative	1.2 (1.2) ± 0.24	

ADCs are given in $\times 10^{-3}$ mm^2. The relationships between the ADCs and the proliferative markers were analyzed by Spearman's rank correlation test; there were no significant correlations (correlation coefficient: –0.206, $P = 0.14$).

Table 3. ADCs obtained by DTI based on rs-EPI regarding prognostic markers

		Mean (median) ± SD	*P*-value
ER	positive	1.1 (1.08) ± 0.25	0.856
	negative	1.09 (1.06) ± 0.18	
PgR	positive	1.08 (1.05) ± 0.25	0.321
	negative	1.14 (1.11) ± 0.19	
HER2	positive	1.08 (1.04) ± 0.16	0.709
	negative	1.11 (1.09) ± 0.25	
Nuclear grade	grades 1, 2	1.11 (1.09) ± 0.25	0.53
	grade 3	1.07 (1.05) ± 0.15	
Intrinsic subtype	luminal type	1.1 (1.06) ± 0.25	0.841
	HER2-positive, TN	1.11 (1.11) ± 0.19	
LN status	positive	1.06 (1.07) ± 0.2	0.44
	negative	1.12 (1.08) ± 0.24	

ADCs are given in $\times 10^{-3}$ mm^2. The relationships between the ADCs and the proliferative markers were analyzed by Pearson's correlation test; there were no significant correlations (correlation coefficient: –0.136, $P = 0.354$).

Mean (median) FA values of the benign and cancer lesions at DTI based on rs-EPI were 0.38 (0.43) and 0.42 (0.41), respectively, and these values were not significantly different ($P = 0.289$).

Our evaluation of the relationship between the FA values and the prognostic markers of invasive breast cancer revealed significant correlations with the ER status, the Ki67 labeling index, the nuclear grade and the intrinsic subtype (Table 4). The ER-negative cancers had significantly lower FA values (median 0.32) than the ER-positive cancers (median 0.46) ($P = 0.017$) (Fig. 2). The FA values were significantly lower with a decreasing Ki67 labeling index (correlation coefficient: –0.327, $P = 0.018$) (Fig. 3).

Table 4. FA values obtained by DTI based on rs-EPI regarding prognostic markers

		Mean (median) ± SD	*P*-value
ER	positive	0.45 (0.46) ± 0.12	0.017
	negative	0.38 (0.32) ± 0.11	
PgR	positive	0.45 (0.45) ± 0.11	0.085
	negative	0.39 (0.36) ± 0.12	
HER2	positive	0.39 (0.36) ± 0.1	0.196
	negative	0.44 (0.44) ± 0.12	
Nuclear grade	grade1, 2	0.45 (0.45) ± 0.11	0.011
	grade 3	0.36 (0.32) ± 0.11	
Intrinsic subtype	luminal type	0.45 (0.45) ± 0.11	0.017
	HER2-positive, TN	0.36 (0.32) ± 0.12	
LN status	positive	0.39 (0.33) ± 0.12	0.1
	negative	0.44 (0.45) ± 0.12	

The FA values are ranged from 0 to 1. The relationships between the FA values and the proliferative markers were analyzed by Spearman's rank correlation test; there were significant correlation (correlation coefficient: –0.327, $P = 0.018$).

The nuclear grade 3 breast cancer had significantly lower FA values (median 0.32) than the nuclear grade 1 or 2 breast cancers (median 0.45) ($P = 0.011$) (Fig. 2). Regarding the intrinsic subtype, the HER2-positive type or TN cancers had significantly lower FA values (median 0.32) compared to the luminal-type cancers (median 0.45) ($P = 0.017$) (Fig. 2).

Representative DW images based on ss-EPI and corresponding DT images based on rs-EPI of benign and breast cancer cases (luminal A-like type cancer and TN cancer) are shown in Figs. 4–6.

Discussion

The results of the present study demonstrate that DTI based on rs-EPI had a superior diagnostic performance for breast cancer compared to DWI based on ss-EPI. The mean ADCs of each benign and breast cancer lesion in the DTI based on rs-EPI were lower than the corresponding ADC obtained by DWI based on ss-EPI. Other studies have reported the same finding.[13,14] Wisner et al. reported that this result is due to reduced blurring artifact in the cancer from nearby normal breast parenchyma[13] because the rs-EPI technique improves lesion conspicuity.[12–14] Wisner et al. also reported that the mean ADC was the same or lower on rs-EPI than on ss-EPI, and this effect was largest in the malignancies.[13] This is the reason that the diagnostic performance of DTI based on rs-EPI is superior to that of DWI based on ss-EPI.

In addition, the improvement of lesion conspicuity enables easier tracing of the ROI of a breast lesion while avoiding the

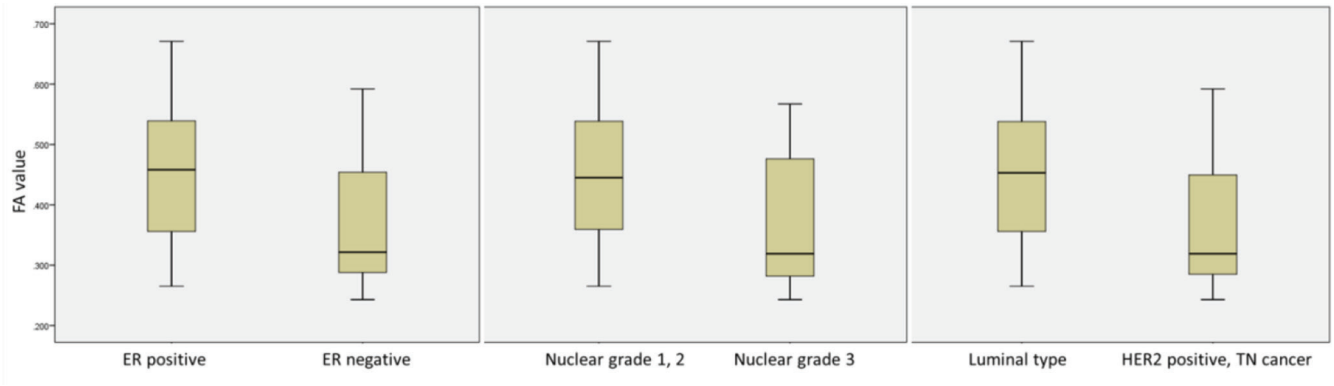

Fig 2. FA values tended to be lower in the ER-negative cancers, cancers with nuclear grade3 and the HER2-positive type or TN cancers.

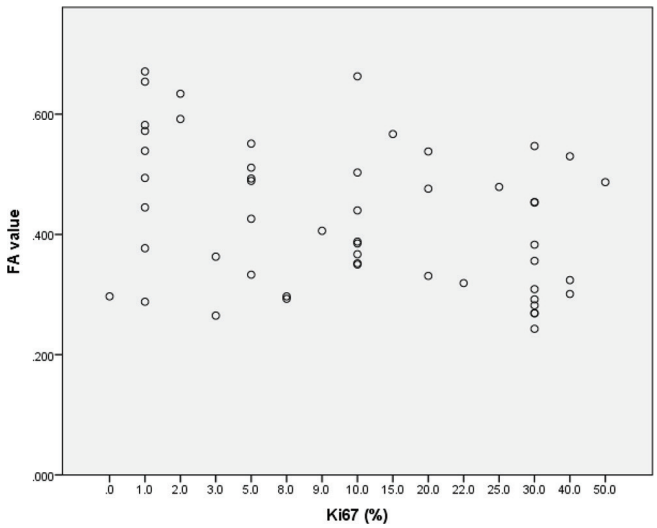

Fig 3. The FA values were significantly lower with a decreasing Ki67 labeling index (correlation coefficient: –0.327, $P = 0.018$).

blurring artifact. This may be another reason for the superior diagnostic performance of DTI based on rs-EPI. In our ROC analysis of the AUCs for diagnostic performance, the AUC based on the rs-EPI (0.924) was greater than that based on ss-EPI (0.897). Bogner et al. reported essentially the same result.[12] They also reported that at the cutoff ADC of 1.25, the sensitivity and specificity for diagnosing breast cancer were 96% and 92%, respectively.[12]

Herein we observed that at the cutoff ADC of 1.338, the sensitivity and specificity for diagnosing breast cancer were 91% and 86%, respectively, which are slightly lower than those reported by Bogner et al. This discrepancy may be due to the differences in MR systems. In our study, a 1.5 T MR system was used; in the Bogner study, a 3 T MR system was used. The signal-to-noise ratio (SNR) of a 3 T MR system is generally higher than that of a 1.5 T system. This higher SNR may have affected the results. Differences in the tumor grade and subtypes in the Bogner study and the present investigation may also have affected the results. However, both studies found that the diagnostic performance of rs-EPI for breast cancer was superior to that of ss-EPI, and it thus appears that rs-EPI is a promising new technique in DWI.

In other studies, the FA values of benign and malignant lesions ranged widely from 0.18 to 0.5 in benign lesions and 0.24 to 0.55 in malignant lesions.[17–20] In the present study, the mean FA values of the benign and malignant breast lesions were 0.38 and 0.42, respectively, and these are within the reported range.

Our evaluation of the relationship between FA values with a variety of prognostic markers of invasive breast cancer revealed significant correlations with the ER status, the proliferative marker, the nuclear grade and the intrinsic subtype. Many other studies reported that the ADC of breast cancer was associated with cellularity, hormone receptor status, HER2 status, a proliferative marker, the tumor grade and the LN status,[25–36] but in the present study there were no significant correlations between the ADCs and prognostic markers in either the DWI based on ss-EPI or the DTI based on rs-EPI. This may be due to differences in the number, the MR systems, the b-values used, the tumor grade and/or the subtype in the various studies.

Our present investigation obtained negative results regarding the relationship between ADCs and prognostic markers, however, there were significant correlations between the FA values and prognostic markers. Our data indicated that the FA value tended to be lower with a decreasing Ki67 labeling index, high nuclear grade, or intrinsic subtype with poor prognosis (i.e., the HER2-positive type or TN cancer). Thus, the FA values tended to be lower with increasing malignant behavior. This tendency may be due to the intratumoral heterogeneity with addition to increasing cellular density.

For example, breast carcinomas with more malignant potential tend to have a high nuclear grade (grade 3). In the classification system used in Japan, nuclear grade 3 shows nuclear pleomorphism with mixed small and large nucleus.[37] This intratumoral heterogeneity may affect the decreasing

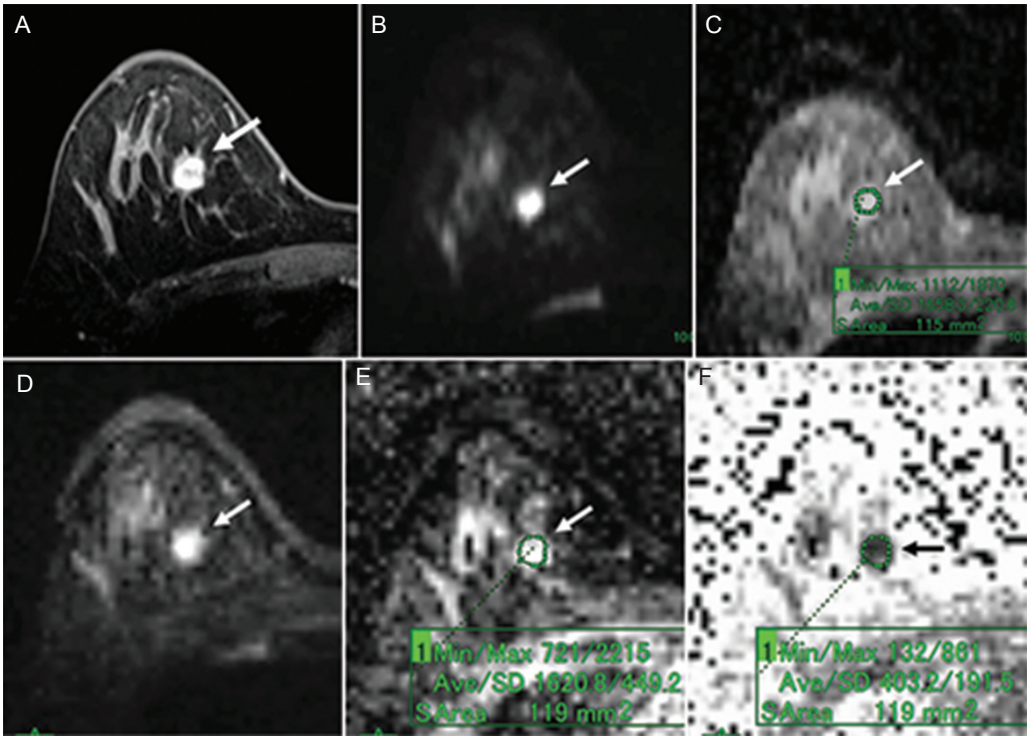

Fig 4. A 39-year-old woman with fibroadenoma. (**A**) Post-contrast, fat-suppressed, axial T_1-weighted image. (**B**) DWI based on ss-EPI. (**C**) ADC map of panel B. (**D**) DTI based on rs-EPI. (**E**) ADC map of panel D. (**F**) FA map of panel D. Post-contrast, fat-suppressed, axial T_1-weighted image shows an oval-shaped mass with a smooth margin and dark internal septation (**A**). The mass shows high signal intensity on both the DWI based on ss-EPI (**B**) and the DTI based on rs-EPI (**D**). On the ADC map of the DWI image, the ADC of the mass was 1.66 (**C**). On the ADC map of the DTI image, the ADC of the mass was 1.62 (**E**). On the FA map, the FA value of the mass was 0.4 (**F**).

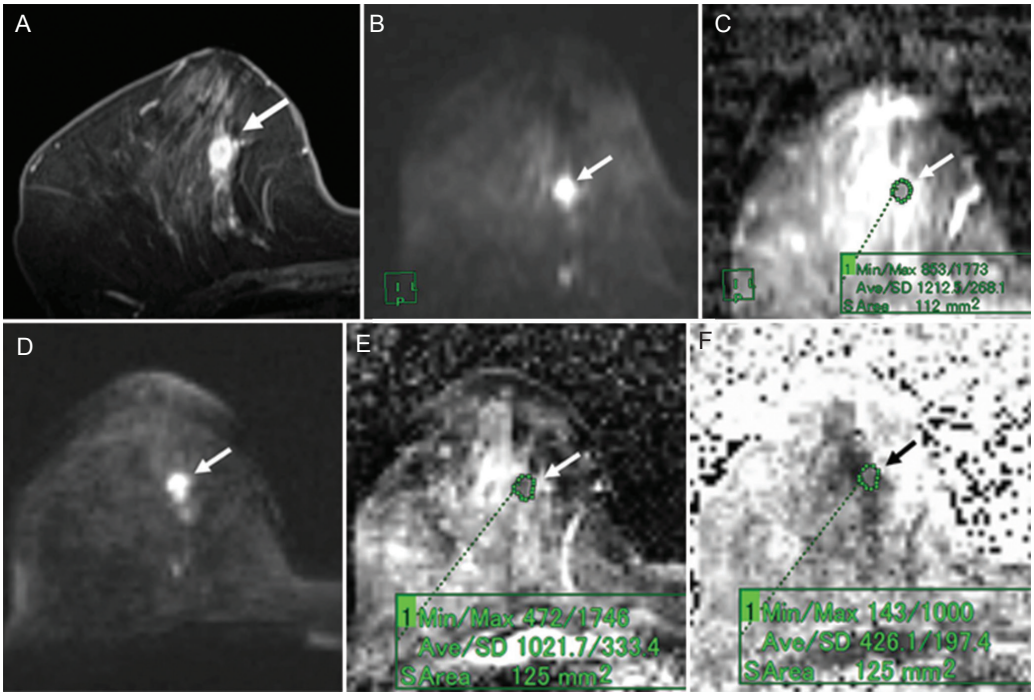

Fig 5. A 66-year-old woman with invasive ductal carcinoma (luminal A-like type). (**A**) Post-contrast, fat-suppressed, axial T_1-weighted image. (**B**) DWI based on ss-EPI. (**C**) ADC map of panel B. (**D**) DTI based on rs-EPI. (**E**) ADC map of panel D. (**F**) FA map of panel D. Post-contrast, fat-suppressed, axial T_1-weighted image shows an oval-shaped mass with a slightly irregular margin and rim enhancement (**A**). The mass shows high signal intensity on both the DWI based on ss-EPI (**B**) and the DTI based on rs-EPI (**D**). On the ADC map of the DWI image, the ADC of the mass was 1.21 (**C**). On the ADC map of the DTI image, the ADC of the mass was 1.02 (**E**). On the FA map, the FA value of the mass was 0.43 (**F**).

anisotropy. With or without micronecrosis, fibrosis and differences in the degree of micronecrosis in the tumor may also affect the anisotropy. Although further studies with detailed pathologic evaluations are needed, we speculate that the FA value may reflect malignant behavior more sensitively compared to standard DWI.

Our study has some limitations. One is the small number of cases (n = 80) in the data set, although a significant result was obtained. More meaningful results could be obtained with greater numbers of cases.

A second limitation is that the fat suppression method used for the DTI based on rs-EPI differed from that used for the DWI based on ss-EPI. We used the CHESS method for fat suppression in the rs-EPI. We first attempted to use the STIR method in the rs-EPI, as this was the method used for the ss-EPI. However, when we used the STIR method for the rs-EPI, the TR became

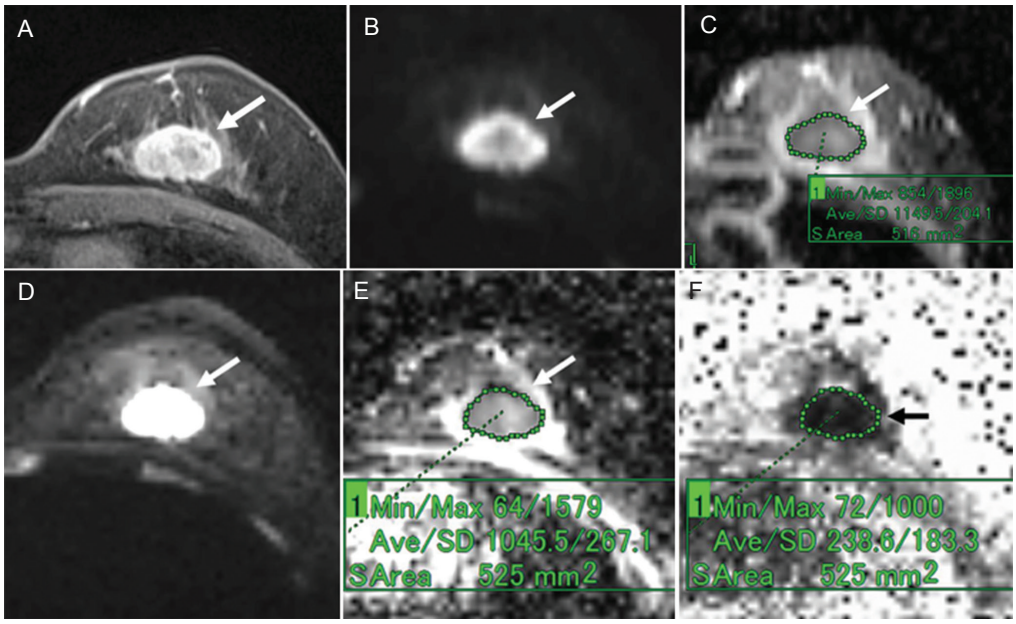

Fig 6. A 59-year-old woman with invasive ductal carcinoma (triple negative cancer). (**A**) Post-contrast, fat-suppressed, axial T_1-weighted image. (**B**) DWI based on ss-EPI. (**C**) ADC map of panel B. (**D**) DTI based on rs-EPI. (**E**) ADC map of panel D. (**F**) FA map of panel D. Post-contrast, fat-suppressed, axial T_1-weighted image shows an oval-shaped mass with a slightly irregular margin and rim enhancement (**A**). The mass shows high signal intensity on both the DWI based on ss-EPI (**B**) and the DTI based on rs-EPI (**D**). On the ADC map of the DWI image, the ADC of the mass was 1.15 (**C**). On the ADC map of the DTI image, the ADC of the mass was 1.05 (**E**). On the FA map, the FA value of the mass was 0.24 (**F**).

longer and as a result, the acquisition time also became longer (almost twice the current acquisition time).

We therefore selected the CHESS method for the rs-EPI to compare the image quality between rs- and ss-EPI with almost-equal acquisition times, taking the clinical effectiveness into consideration. This difference may have influenced our results. In the future, if the STIR method can be selected for rs-EPI with the same acquisition time as that for ss-EPI, evaluations using the STIR fat suppression method for both the rs-EPI and ss-EPI techniques should be conducted. A third study limitation is the lack of a detailed pathologic correlation.

In conclusion, DTI based on rs-EPI showed a superior diagnostic performance for breast cancer compared to DWI based on ss-EPI. The FA values were more closely correlated with several prognostic factors (ER, the Ki67 labeling index, the nuclear grade and the intrinsic subtype) for invasive breast cancer compared to the ADCs.

Conflicts of Interest

Yoshiaki Komori: Employee of Siemens Japan K.K.

All other authors declare that they have no conflicts of interest.

References

1. Fischer U, Kopka L, Brinck U, Korabiowska M, Schauer A, Grabbe E. Prognostic value of contrast-enhanced MR mammography in patients with breast cancer. Eur Radiol 1997; 7:1002–1005.
2. Fischer U, Kopka L, Grabbe E. Breast carcinoma: effect of preoperative contrast-enhanced MR imaging on the therapeutic approach. Radiology 1999; 213:881–888.
3. Van Goethem M, Schelfout K, Kersschot E, et al. MR mammography is useful in the preoperative locoregional staging of breast carcinomas with extensive intraductal component. Eur J Radiol 2007; 62:273–282.
4. Lehman CD, Gatsonis C, Kuhl CK, et al. MRI evaluation of the contralateral breast in women with recently diagnosed breast cancer. N Engl J Med 2007; 356:1295–1303.
5. Orel SG, Schnall MD. MR imaging of the breast for the detection, diagnosis, and staging of breast cancer. Radiology 2001; 220:13–30.
6. Yamaguchi K, Schacht D, Sennett CA, et al. Decision making for breast lesions initially detected at contrast-enhanced breast MRI. AJR Am J Roentgenol 2013; 201:1376–1385.
7. Woodhams R, Ramadan S, Stanwell P, et al. Diffusion-weighted imaging of the breast: principles and clinical applications. Radiographics 2011; 31:1059–1084.
8. Kuroki Y, Nasu K, Kuroki S, et al. Diffusion-weighted imaging of breast cancer with the sensitivity encoding technique: analysis of the apparent diffusion coefficient value. Magn Reson Med Sci 2004; 3:79–85.
9. Matsubayashi RN, Fujii T, Yasumori K, Muranaka T, Momosaki S. Apparent diffusion coefficient in invasive ductal breast carcinoma: correlation with detailed histologic features and the enhancement ratio on dynamic contrast-enhanced MR images. J Oncol 2010; 2010. doi: 10.1155/2010/821048..
10. Partridge SC, DeMartini WB, Kurland BF, Eby PR, White SW, Lehman CD. Quantitative diffusion-weighted imaging as an adjunct to conventional breast MRI for improved positive predictive value. AJR Am J Roentgenol 2009; 193:1716–1722.
11. Kuroki Y, Nasu K. Advances in breast MRI: diffusion-weighted imaging of the breast. Breast Cancer 2008; 15:212–217.
12. Bogner W, Pinker-Domenig K, Bickel H, et al. Readout-segmented echo-planar imaging improves the diagnostic performance of diffusion-weighted MR breast examinations at 3.0 T. Radiology 2012; 263:64–76.
13. Wisner DJ, Rogers N, Deshpande VS, et al. High-resolution diffusion-weighted imaging for the separation of benign

from malignant BI-RADS 4/5 lesions found on breast MRI at 3T. J Magn Reson Imaging 2014; 40:674–681.
14. Kim YJ, Kim SH, Kang BJ, et al. Readout-segmented echo-planar imaging in diffusion-weighted mr imaging in breast cancer: comparison with single-shot echo-planar imaging in image quality. Korean J Radiol 2014; 15:403–410.
15. Porter DA, Heidemann RM. High resolution diffusion-weighted imaging using readout-segmented echo-planar imaging, parallel imaging and a two-dimensional navigator-based reacquisition. Magn Reson Med 2009; 62:468–475.
16. Partridge SC, Murthy RS, Ziadloo A, White SW, Allison KH, Lehman CD. Diffusion tensor magnetic resonance imaging of the normal breast. Magn Reson Imaging 2010; 28: 320–328.
17. Partridge SC, Ziadloo A, Murthy R, et al. Diffusion tensor MRI: preliminary anisotropy measures and mapping of breast tumors. J Magn Reson Imaging 2010; 31:339–347.
18. Baltzer PA, Schäfer A, Dietzel M, et al. Diffusion tensor magnetic resonance imaging of the breast: a pilot study. Eur Radiol 2011; 21:1–10.
19. Tsougos I, Svolos P, Kousi E, et al. The contribution of diffusion tensor imaging and magnetic resonance spectroscopy for the differentiation of breast lesions at 3T. Acta Radiol 2014; 55:14–23.
20. Cakir O, Arslan A, Inan N, et al. Comparison of the diagnostic performances of diffusion parameters in diffusion weighted imaging and diffusion tensor imaging of breast lesions. Eur J Radiol 2013; 82:e801–806.
21. Wang Y, Zhang XP, Li YL, et al. Optimization of the parameters for diffusion tensor magnetic resonance imaging data acquisition for breast fiber tractography at 1.5 T. Clin Breast Cancer 2014; 14:61–67.
22. Tagliafico A, Rescinito G, Monetti F, et al. Diffusion tensor magnetic resonance imaging of the normal breast: reproducibility of DTI-derived fractional anisotropy and apparent diffusion coefficient at 3.0 T. Radiol Med 2012; 117:992–1003.
23. Nissan N, Furman-Haran E, Shapiro-Feinberg M, Grobgeld D, Degani H. Diffusion-tensor MR imaging of the breast: hormonal regulation. Radiology 2014; 271:672–680.
24. Goldhirsch A, Winer EP, Coates AS, et al. Personalizing the treatment of women with early breast cancer: highlights of the St Gallen International Expert Consensus on the Primary Therapy of Early Breast Cancer 2013. Ann Oncol 2013; 24:2206–2223.
25. De Felice C, Cipolla V, Guerrieri D, et al. Apparent diffusion coefficient on 3.0 Tesla magnetic resonance imaging and prognostic factors in breast cancer. Eur J Gynaecol Oncol 2014; 35:408–414.
26. Park SH, Choi HY, Hahn SY. Correlations between apparent diffusion coefficient values of invasive ductal carcinoma and pathologic factors on diffusion-weighted MRI at 3.0 Tesla. J Magn Reson Imaging 2015; 41:175–182.
27. Mori N, Ota H, Mugikura S, et al. Luminal-type breast cancer: correlation of apparent diffusion coefficients with the Ki-67 labeling index. Radiology 2015; 274:66–73.
28. Woodhams R, Kakita S, Hata H, et al. Diffusion-weighted imaging of mucinous carcinoma of the breast: evaluation of apparent diffusion coefficient and signal intensity in correlation with histologic findings. AJR Am J Roentgenol 2009; 193:260–266.
29. Martincich L, Deantoni V, Bertotto I, et al. Correlations between diffusion-weighted imaging and breast cancer biomarkers. Eur Radiol 2012; 22:1519–1528.
30. Belli P, Costantini M, Bufi E, et al. Diffusion magnetic resonance imaging in breast cancer characterisation: correlations between the apparent diffusion coefficient and major prognostic factors. Radiol Med 2015; 120:268–276.
31. Yoshikawa MI, Ohsumi S, Sugata S, et al. Relation between cancer cellularity and apparent diffusion coefficient values using diffusion-weighted magnetic resonance imaging in breast cancer. Radiat Med 2008; 26:222–226.
32. Choi SY, Chang YW, Park HJ, Kim HJ, Hong SS, Seo DY. Correlation of the apparent diffusion coefficiency values on diffusion-weighted imaging with prognostic factors for breast cancer. Br J Radiol 2012; 85:e474–e479.
33. Cipolla V, Santucci D, Guerrieri D, Drudi FM, Meggiorini ML, de Felice C. Correlation between 3T apparent diffusion coefficient values and grading of invasive breast carcinoma. Eur J Radiol 2014; 83:2144–2150.
34. Kamitani T, Matsuo Y, Yabuuchi H, et al. Correlations between apparent diffusion coefficient values and prognostic factors of breast cancer. Magn Reson Med Sci 2013; 12:193–199.
35. Razek AA, Gaballa G, Denewer A, Nada N. Invasive ductal carcinoma: correlation of apparent diffusion coefficient value with pathological prognostic factors. NMR Biomed 2010; 23:619–623.
36. Kim SH, Cha ES, Kim HS, et al. Diffusion-weighted imaging of breast cancer: correlation of the apparent diffusion coefficient value with prognostic factors. J Magn Reson Imaging 2009; 30:615–620.
37. The Japanese Breast Cancer Society. [General rules for clinical and pathological recording of breast cancer 17th ed]. Kanehara: Tokyo; 2012 (in Japanese).